AIP Journal of Applied Physics

Tunable configurational anisotropy of concave triangular nanomagnets

Kasuni Nanayakkara, Ivan S. Vasil'evskii, Igor S. Eremin, Olga S. Kolentsova, Nikolay I. Kargin, Alexander Anferov, and Alexander Kozhanov

Citation: Journal of Applied Physics **119**, 233906 (2016); doi: 10.1063/1.4954162
View online: http://dx.doi.org/10.1063/1.4954162
View Table of Contents: http://scitation.aip.org/content/aip/journal/jap/119/23?ver=pdfcov
Published by the AIP Publishing

Tunable configurational anisotropy of concave triangular nanomagnets

Kasuni Nanayakkara,[1,2] Ivan S. Vasil'evskii,[3] Igor S. Eremin,[3] Olga S. Kolentsova,[3] Nikolay I. Kargin,[3] Alexander Anferov,[1] and Alexander Kozhanov[1,2,a)]
[1]*Department of Physics and Astronomy, Georgia State University, Atlanta, Georgia 30303, USA*
[2]*Center for Nano Optics, Georgia State University, Atlanta, Georgia 30303, USA*
[3]*National Research Nuclear University MEPhI, Moscow, Russia*

(Received 1 March 2016; accepted 6 June 2016; published online 21 June 2016)

Shape and dimension variation effects on the configurational anisotropy and magnetization ground states of single domain triangular nano-magnets are investigated using micromagnetic simulations and magnetic force microscopy. We show that introducing concavity or elongating vertexes stabilize the Y magnetization ground states of triangular nanomagnets. A phenomenological model relating the magnetization anisotropy and triangle geometry parameters is developed. MFM imaging reveals shape defined buckle and Y ground states that are in good agreement with numeric simulations. Concavity and vertex extrusion allow for the form-ruled magnetization ground state engineering in the shapes with higher orders of symmetry. *Published by AIP Publishing.*
[http://dx.doi.org/10.1063/1.4954162]

Magnetic nano-structures are well suited as a basic building block for the non-volatile memory and logic applications.[1–5] Majority of the existing memory applications are based on the nanomagnets that exhibit uniaxial magnetic anisotropy with two stable magnetization ground states.[4,6] Soft magnetic materials enable the shape anisotropy defined single domain ground state of the magnetic element at nano-scale.

A non-uniform magnetization ground state is observed in more complex shapes.[7] Configurational anisotropy defines the magnetization ground state. In nano-magnets with higher order of symmetry, such as triangles and squares, the symmetry of the nanomagnet shape defines the magnetization configuration that has the same order of symmetry as its shape.[8] Triangular nanomagnet can relax into either buckle or Y magnetization ground states dependent on its geometry.[9]

Stability of these states was intensively studied as a function of the triangle lateral dimension and thickness. It was demonstrated that for the equilateral triangle with sharp vertexes, the Y state dominates within a well-defined range of triangle dimensions. In particular, all sharp Permalloy triangles with a side length less than 100–150 nm should relax into Y ground state, while all larger nanomagnets demonstrate more stable buckle state. As lateral dimensions of a triangular nanomagnet are increased to micron-scale, the vortex ground state becomes more stable.[10]

Recently, a non-volatile logic device utilizing the Y ground state of a nanomagnetic triangle, Spin Torque Triad (STT), was proposed.[11] The magnetization orientation within the of the triangle vertexes directed radially inwards or outwards of the triangle center is used to store 3 bits of information in Boolean form (1 bit per triangle vertex). The input is written by locally switching the triangle magnetization within the two triangle vertexes (2 inputs) which results in switching of the triangle ground state. The local magnetization alignment of the third triangle vertex thus switched follows either NAND or NOR logic gate operation and serves as an output. Energy per operation and operational speed of such device are strongly dependent on the stability of the Y ground state. Recent study revealed that introduction of corner rounding to the triangle typically occurring during fabrication process results in a stable buckle state,[12] magnetization orientation of which is unfavorable for the STT operation.

In this paper, we use micromagnetic simulations and magnetic force microscopy to investigate the shape variation effect on the configurational anisotropy and magnetization ground state stability of the triangular nanomagnets. It was shown previously that varying the concavity of rectangular nanomagnets can be used to manipulate the energy barrier between the ground states of the rectangular magnetic elements.[13,14] In our work, we demonstrate that by varying the amount of concavity and triangle vertex extrusion length, either buckle or Y magnetization configurations can be stabilized and the configurational anisotropy can be effectively controlled resulting in tunable switching energy barrier.

Micromagnetic simulations of the field modulated torque magnetometry[9] on concave nanomagnetic triangles with varying concavity and vertex extrusion length using LLG micromagnetic simulator software package[15] were carried out. Permalloy ($Ni_{80}Fe_{20}$) was chosen as the magnetic material. Following simulation parameters were used: saturation magnetization $M_s = 860\,\text{emu/cm}^3$, no anisotropy, mesh size 1 nm, and exchange stiffness constant $A = 1.05\,\text{erg/cm}^3$.

Geometry of concave triangles used in micromagnetic simulations is schematically shown in Fig. 1. Equilateral triangle with side length a is used as a base. Radius R_v of the three circles inscribed into the equilateral triangle vertexes defines the corner rounding. Concavity is introduced by the circles of radius R_c that make tangential contact with the corner rounding circles. As R_c is decreased, the amount of concavity increases. When condition $R_c = a - (1 + 2/\sqrt{3})R_v$ is satisfied, the point of corner rounding contact with these circles reaches the tangential line, parallel to the triangle axis. Further decrease of the concavity radius is done by

a)Electronic mail: akozhanov@gsu.edu

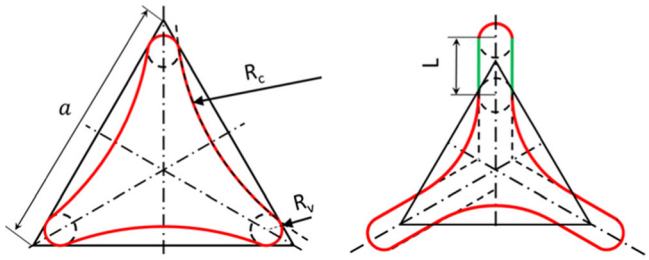

FIG. 1. Schematic of the nano-magnetic triangle geometry for the concavity (left) and vertex extrusion (right) variation.

keeping the concavity-defining circle tangent to the lines, parallel to the triangle symmetry axis which are also tangent to the corner rounding circles. That results in concave triangles with elongated vertexes, width of which is defined by the diameter of the corner rounding circles. We define the vertex extrusion length L as a distance on which the corner rounding circles are shifted along the triangle symmetry axes from their original positions. Base triangle side length was varied within $50\,\text{nm} < a < 500\,\text{nm}$. Its thickness varied in the 5 to 15 nm range. For each nanomagnet, length and thickness, concavity radius varied starting from straight sides to a star-like structure with zero radius of concavity. Triangle symmetry axis was aligned at 75° to the grid for comparable amount of roughness due to pixilation on all triangle sides.

A constant in-plane magnetic field of $H_{dc} = 1000\,\text{Oe}$ large enough to saturate the studied nanomagnet was applied at an angle θ. Magnetization tilt off the θ direction $\pm\Delta\theta$ caused by the small modulating field $H_{ac} = 10\,\text{Oe}$ applied at $\pm 90°$ with respect to H_{dc} was measured. The configurational anisotropy total field was calculated using the following expression:[9]

$$H_{tot}(\theta) = H_a + H_{dc} = \frac{H_{ac}}{\Delta\theta}, \tag{1}$$

where H_a anisotropy field, θ varied in the range 0°–360°. More detailed description of the torque magnetometry used in simulations can be found in the literature.[9]

Typical results of anisotropy simulations for the triangles with various amounts of concavity are shown in Fig. 2. All $H_{tot}(\theta)$ curves show multiple peaks that are aligned either along the triangle sides (indicating stable buckle state) or along its symmetry axes (indicating stable Y state). For the triangle with vanishing concavity (straight sides, $R_c = 200a$), H_{tot} maxima aligned along the directions parallel to the triangle sides ($\theta = 15° + k\pi/3$, $k \in \mathbb{Z}$) are observed. That indicates of the buckle ground state, which is typical for straight side triangles with rounded corners.[12] For the triangle with $R_c = 1.4a$, the difference between buckle (along the side) and Y (along the symmetry axis) state H_{tot} values vanishes; this triangle randomly relaxes into buckle or Y ground states in the absence of external biasing fields. With further increase of concavity (decrease of R_c), amplitude of $\theta = 45° + k\pi/3$ peaks is growing which is indicative of the Y-state stability increase. It is known that the stable ground state type can depend on the H_{dc} values used to perform torque magnetometry.[9] Varying H_{dc} did not reveal any changes in the observed ground states for each of the triangle dimensions.

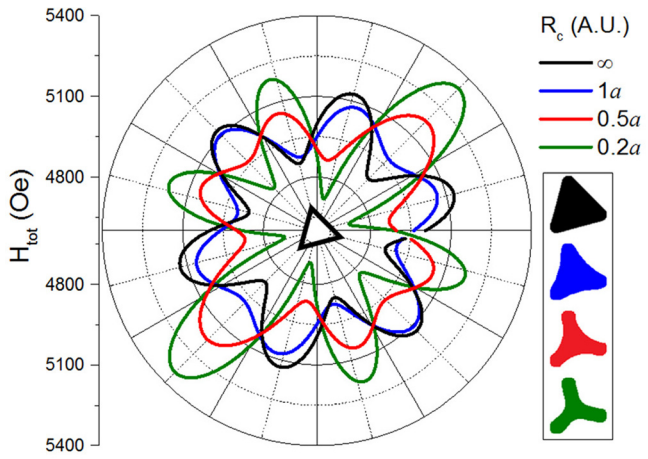

FIG. 2. Total anisotropy field dependence on the in plane direction. Triangle side length 100 nm, corner radius 10 nm, and concavity radius R_c are shown in the graph legend in units of triangle base side length a. Inset shows the triangle geometry used for the simulation.

The anisotropy energy U was calculated following the configurational anisotropy model for symmetrical nanomagnets developed by Cowburn *et al.*:[8]

$$U = \frac{2M_s H_a V}{n^2}, \tag{2}$$

where V is the nanomagnet volume and n its rotational symmetry order. The anisotropy energy U is plotted in Fig. 3 as a function of square root of the surface area. As the concavity radius decreases, the anisotropy energy of the buckle state decreases. For triangles with concavity radius $R_c \leq 1.4a$, Y state is more stable with anisotropy energy increasing as the concavity radius is decreased. Cowburn *et al.* revealed a phenomenological relationship between the nanomagnet surface area and the anisotropy energy: $U = C(\sqrt{Area} + l_0)$, where C and l_0 are constants when $U > 0$. We adopted the anisotropy field and anisotropy energy sign convention used in papers by Cowburn *et al.*[8,9] Our results indicate that for negative U (buckle state), the energy barrier does increase with the square root of the area; however, as concavity radius decreases (followed by area), U becomes positive (Y state) and increases. These results indicate that for a constant triangle side length, its anisotropy energy is governed by concavity variation rather than the nanomagnet volume or surface area variation.

In order to evaluate the effect of the triangular nanomagnet vertex extrusion, simulations of the anisotropy energy in directions of buckle ($\theta = 45°$) and Y ($\theta = 75°$) states were carried out. Field variation approach was used: the maxima position of the transverse susceptibility versus H_{dc} indicated the anisotropy field H_a for each direction. A 5 nm thick triangle with the following parameters was used as a base: $a = 55\,\text{nm}$, $R_v = 5\,\text{nm}$, $R_c = 50\,\text{nm}$. In the absence of external magnetic field, its magnetization relaxed into the Y state, thus defining hard axis at $\theta = 45°$ direction and easy axis at the $\theta = 75°$. The energy barrier ΔU between two neighboring stable Y states is defined by the difference in the anisotropy energies measured along the hard and easy directions.

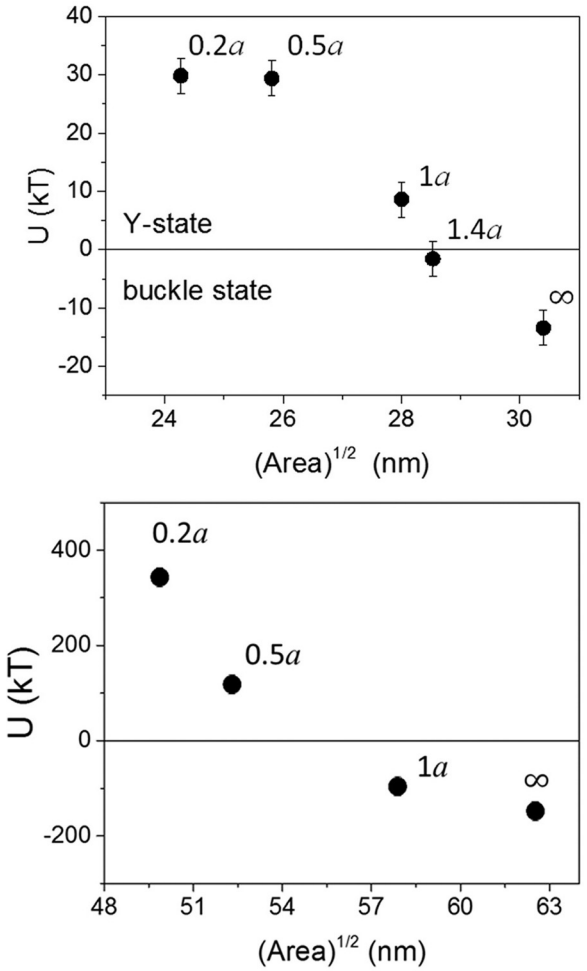

FIG. 3. Anisotropy energy dependence on the amount of concavity of triangular nanomagnet. Concavity radius R_c values are shown next to each data point in units of the base triangle side length a for $a = 50$ nm (top) and $a = 100$ nm (bottom). Error bars originate form the angular variation discretization.

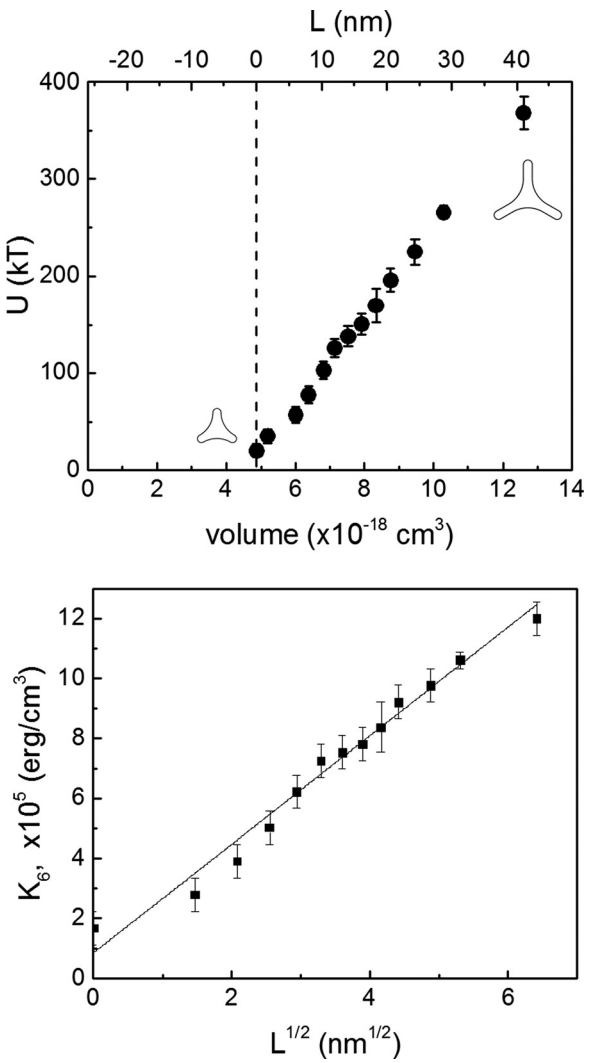

FIG. 4. Anisotropy energy (top) and anisotropy constant (bottom) of the triangular nanomagnet with the base side length $a = 55$ nm. Error bars originate form the magnetic field variation discretization.

ΔU of the triangle with non-extruded vertexes is $(15 \pm 2)kT$. Micromagnetic simulations carried out for a triangles with vertex extrusion length varied from 0 to 41 nm ($L = 0.75a$) are summarized in Fig. 4. The anisotropy energy increases linearly with the nanomagnet volume V. Calculated anisotropy constant K_6 demonstrates linear behavior as a function of square root of the vertex extrusion length L (Fig. 4). At $L = 0$, the anisotropy energy is defined by the triangle concavity which can be summarized as

$$U_{tot} = U_{conc} + U_{extr} = (K_6^0 + C_L\sqrt{L})V \sin^2(3\theta). \quad (3)$$

U_{conc} and U_{extr} are the anisotropy energy contributions defined by the concavity and vertex extrusion variation. K_6^0 is the anisotropy constant defined by the triangle core dimensions (a, r, R_c), V is the nanomagnet volume, C_L is the phenomenological constant, indicating the slope of the $K_6(\sqrt{L})$ curve (Fig. 4) defined by the thickness and width of the triangle vertex extrusions.

The vertex extrusion offers a convenient control over the nanomagnet ground state stability from technological point of view. Controlling the vertex extrusion length provides a much wider range of the anisotropy energy control than does the shape of the triangle.

Effect of triangular nanomagnet shape variation on its ground state stability was investigated experimentally using the magnetic force microscopy.

Nanomagnetic triangles of varying shapes and dimensions were fabricated as follows. Electron beam lithography using the PMMA resist followed by the lift-off technique was used to define the $(25 \times 25)\mu m^2$ arrays of triangles with varying shapes and dimensions on a silicon substrate. A 15 nm thick $Ni_{80}Fe_{20}$ film was deposited on top of 5 nm Ti adhesion layer and capped with 2 nm of Cu using electron beam evaporation technique. Scanning electron micrographs of typical fabricated triangular nanomagnets are shown in Fig. 5. Veeco Multimode V atomic force microscope was used to perform the magnetic force microscopy on the fabricated samples using the conical high resolution MFM probes with less than 15 nm tip radius, approximately 125 Oe coercivity and 80 emu/cc remanence magnetization. The scans were performed at the lift heights varying in the range 10–40 nm and at different sample orientations to rule out

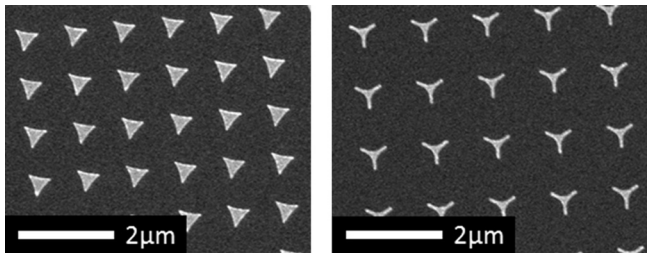

FIG. 5. SEM of typical fabricated structures: concave triangles (left) and triangles with extruded vertexes (right).

tip-induced perturbations. MFM scans were performed in the absence of biasing magnetic field on "as fabricated" triangular nanomagnet arrays as well as after subjecting them to the biasing magnetic field saturating nanomagnets in various directions to ensure the stability of observed magnetic configurations.

Examples of the MFM images recorded on the fabricated samples are shown in Fig. 6. In order to analyze the MFM images, micromagnetic simulations of the triangle ground states were carried out. The triangle base length, corner rounding, and concavity radius were determined from SEM micrographs and used to run micromagnetic simulations. Nanomagnet ground states were simulated by magnetization relaxation from initial state with random magnetization

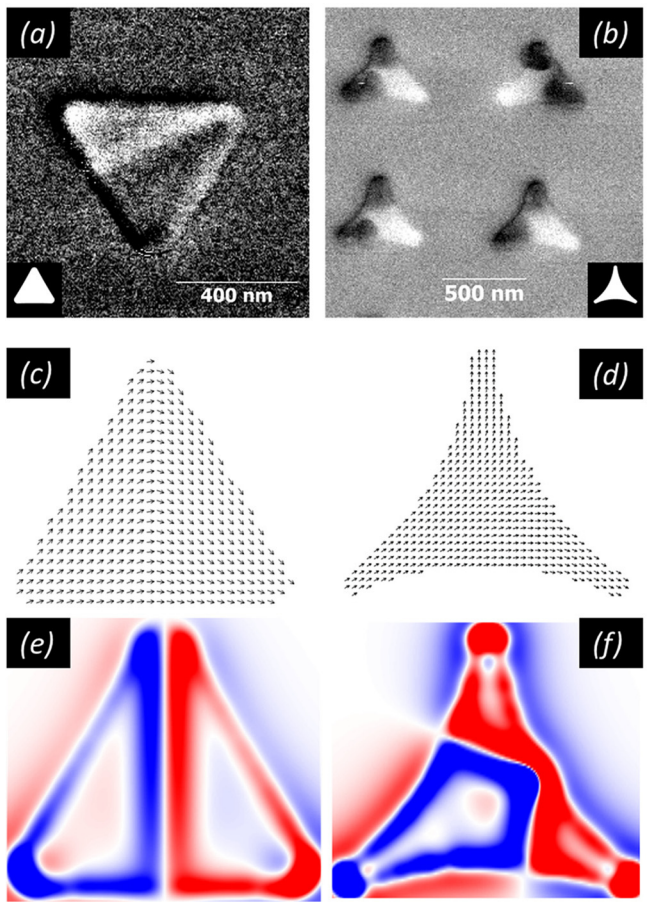

FIG. 6. MFM images, simulated magnetization alignment, and corresponding simulated MFM images of triangles with $a = 500\,\text{nm}$, straight sides, $R_v = 40\,\text{nm}$ ((a), (c), and (e)) and concave sides, $R_c = 500\,\text{nm}$, $R_v = 20\,\text{nm}$ ((b), (d), and (f)). Insets in MFM images are the triangle design patterns used for the structure fabrication.

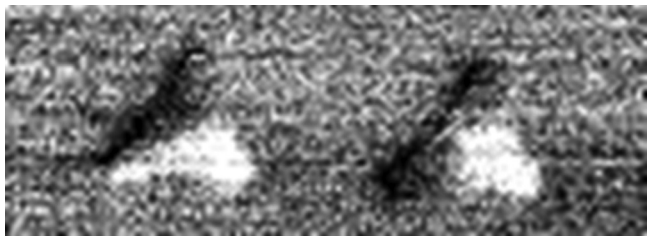

FIG. 7. MFM image of two neighboring triangles relaxed into buckle (left) and Y (right) states. $a = 500\,\text{nm}$, $R_v = 20\,\text{nm}$, and $R_c = 500\,\text{nm}$.

orientation in the absence of external biasing fields. Results of ground state simulations are shown in Figs. 6(c) and 6(d). The MFM signal is given by a phase shift of the cantilever oscillations which is proportional to the second order derivative of the perpendicular stray magnetic field component $(\partial^2 H_z/\partial z^2)$.[16] For the simulated magnetization, configuration $(\partial^2 H_z/\partial z^2)$ was calculated at 20 nm distance above the surface. Images thus obtained are shown in Figs. 6(e) and 6(f). Simulated images mimic the experimentally obtained MFM images which suggests that the magnetization configurations shown in Fig. 6 are the ones imaged by MFM. As a result, MFM images confirm that the Y ground state is stabilized by introducing concavity. MFM scans and micromagnetic simulations of nanomagnets with magnetization relaxing from a saturated state with initial magnetization defined by in-plane biasing magnetic field applied in various directions did not reveal any dependence of the magnetization configuration on the biasing field history.

The same imaging procedure was repeated on the arrays on non-interacting triangular nanomagnets with concavity radius varying within the range $0.2a \leq R_c \leq 10a$. Statistical data was gathered on approximately 100 triangles for each parameter set. All triangles with concavity radius less than the side length relaxed into a stable buckle state. Triangles with $R_c \approx a$ demonstrated a mixture of both buckle and Y states observed with equal probability. MFM image demonstrating the two neighboring triangles of the same dimension exhibiting the buckle and Y ground states is shown in Fig. 7. As the concavity radius is decreased, triangle switched from more stable buckle into the Y ground state. These results are in good agreement with the micromagnetic simulations discussed above.

In summary, the concavity and vortex extrusion variation effects on the nanomagnetic triangle ground state stability were studied. Decreasing the concavity radius (increasing the amount of concavity) results in decrease of the buckle state and increase of the Y magnetization ground state stability. The magnetization switching energy barrier can be controlled by varying the concavity radius and the vertex extrusion length. Micromagnetic simulations indicate that the transition from the buckle into the Y ground state happens when the concavity radius is approximately equal to the triangle side length. This is confirmed by the MFM imaging of imaging the arrays of non-interacting triangular nanomagnets. Varying the vertex extrusion length allows for controllable variation of the triangle ground state switching energy barrier. The phenomenological relationship between the anisotropy constant and triangle vertex extrusion length was found. We

demonstrated that the magnetization switching energy barrier can be varied in a wide range that makes the triangular nanomagnets practical for use in nano-magnetic logic and memory devices.

This work was partially supported by Georgia State University.

[1]R. Cowburn and M. Welland, Science **287**, 1466 (2000).
[2]G. Csaba, G. H. Bernstein, A. Orlov, M. T. Niemier, X. S. Hu, and W. Porod, *CMOS and Beyond: Logic Switches for Terascale Integrated Circuits* (Cambridge University Press, 2015), p. 301.
[3]A. Haldar and A. O. Adeyeye, ACS Nano **10**, 1690 (2016).
[4]T. Kawahara, K. Ito, R. Takemura, and H. Ohno, Microelectron. Reliab. **52**, 613 (2012).
[5]D. E. Nikonov and I. A. Young, Proc. IEEE **101**, 2498 (2013).
[6]R. C. Sousa and I. L. Prejbeanu, C. R. Phys. **6**, 1013 (2005).
[7]R. P. Cowburn, A. O. Adeyeye, and M. E. Welland, Phys. Rev. Lett. **81**, 5414 (1998).
[8]R. P. Cowburn, J. Phys. D: Appl. Phys. **33**, R1 (2000).
[9]D. K. Koltsov, R. P. Cowburn, and M. E. Welland, J. Appl. Phys. **88**, 5315 (2000).
[10]S. Yakata, M. Miyata, S. Nonoguchi, H. Wada, and T. Kimura, Appl. Phys. Lett. **97**, 222503 (2010).
[11]A. Kozhanov, S. Allen, and C. Palmstrom, "Spin transfer torque triad for non-volatile logic gates," U.S. patent 8,198,919 (2012).
[12]L. Thevenard, H. T. Zeng, D. Petit, and R. P. Cowburn, J. Appl. Phys. **106**, 063902 (2009).
[13]D. Koltsov and M. Welland, J. Appl. Phys. **94**, 3457 (2003).
[14]B. Lambson, Z. Gu, M. Monroe, S. Dhuey, A. Scholl, and J. Bokor, Appl. Phys. A **111**, 413 (2013).
[15]M. Scheinfein, See http://llgmicro.home.mindspring.com for LLG micromagnetic simulator, 1997.
[16]U. Hartmann, Phys. Lett. A **137**, 475 (1989).